Supplementary information for: Conformational stability adaptation of a double-stranded RNA binding domain to transfer RNA ligand

Charles Bou-Nader[1], Ludovic Pecqueur[1], Pierre Barraud[2], Marc Fontecave[1], Carine Tisné [2], Sophie Sacquin-Mora[3], and Djemel Hamdane[1*]

[1]Laboratoire de Chimie des Processus Biologiques, CNRS-UMR 8229, Collège De France, Université Pierre et Marie Curie, 11 place Marcelin Berthelot, 75231 Paris Cedex 05, France

[2]Institut de biologie physico-chimique (IBPC), UMR 8261 CNRS/Université Paris Diderot, 13 rue Pierre et Marie Curie, Paris 75005, France.

[3]Laboratoire de Biochimie Théorique, CNRS UPR9080, Institut de Biologie Physico-Chimique, 13 rue Pierre et Marie Curie, 75005, Paris, France.

*To whom correspondence should be addressed: Djemel Hamdane, Email : djemel.hamdane@college-de-france.fr
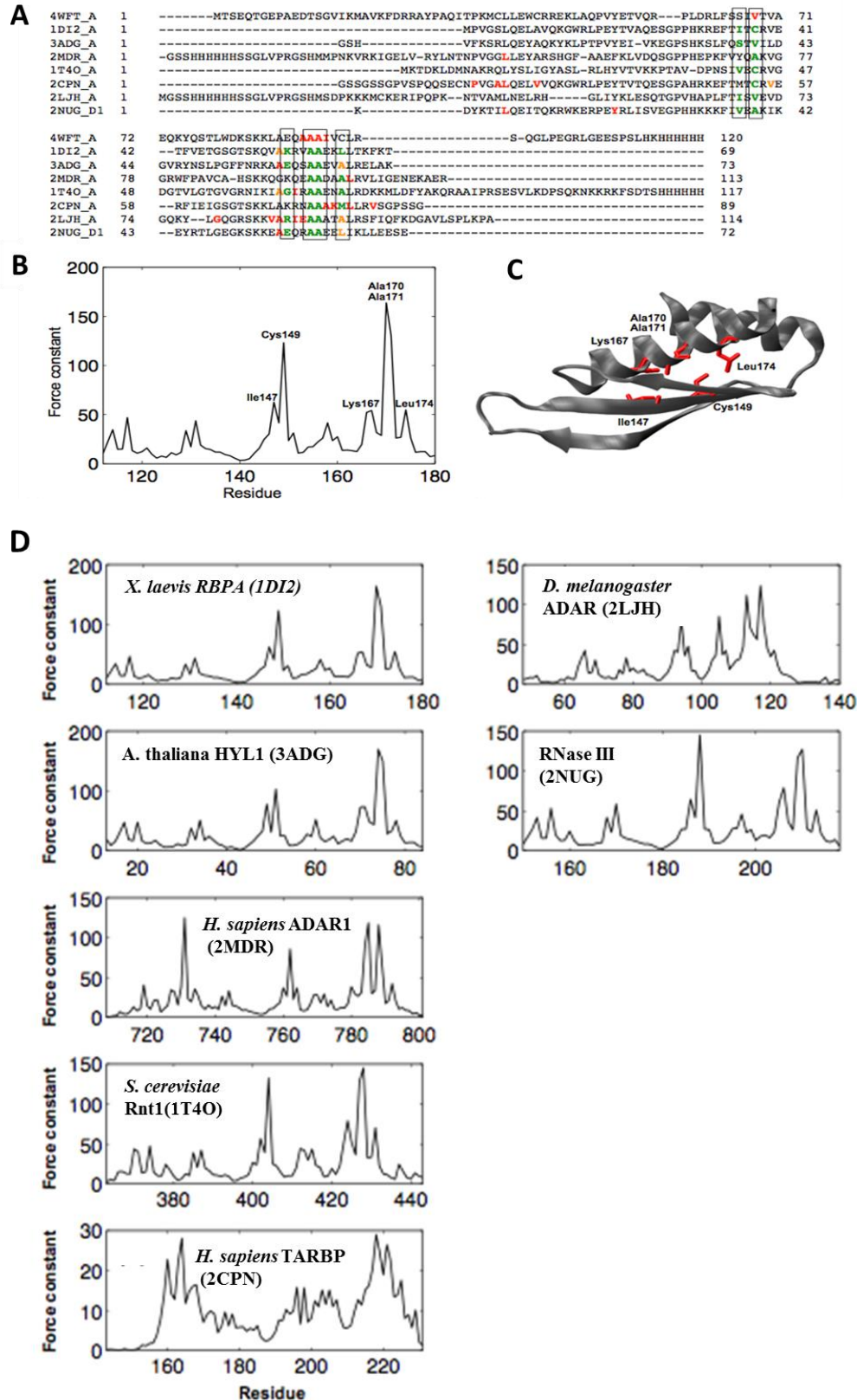
A

```
4WFT_A   1  -------MTSEQTGEPAEDTSGVIKMAVKFDRRAYPAQITPKMCLLEWCRREKLAQPVYETVQR---PLDRLFSSVTVA    71
1DI2_A   1  --------------------------------------------MPVGSLQELAVQKGWRLPEYTVAQESGPPHKREFTITCRVE    41
3ADG_A   1  -----------------GSH-------------VFKSRLQEYAQKYKLPTPVYEI-VKEGPSHKSLFQSTVILD    43
2MDR_A   1  -GSSHHHHHHSSGLVPRGSHMMPNKVRKIGELV-RYLNTNPVGGLLEYARSHGF-AAEFKLVDQSGPHEPKFVYQAKVG    77
1T4O_A   1  ----------------MKTDKLDMNAKRQLYSLIGYASL-RLHYVTVKKPTAV-DPNSIVBCRVG    47
2CPN_A   1  ----------------GSSGSSGPVSPQQSECNPVGALVVQKGWRLPEYTVTQESGPAHRKEFTMTCRVE    57
2LJH_A   1  MGSSHHHHHHSSGLVPRGSHMSDPKKKMCKERIPQPK--NTVAMLNELRH-----GLIYKLESQTGPVHAPLFTISVEVD    73
2NUG_D1  1  ------------------------K--------DYKTILQEITQKRWKERPEYRLISVEGPHHKKKFIVRAKIK    42

4WFT_A   72  EQKYQSTLWDKSKKLAEQAAAIVCLR-------------------S-QGLPEGRLGEESPSLHKHHHHHH   120
1DI2_A   42  --TFVETGSGTSKQVAKRVAAEKLLTKFKT------------------------------   69
3ADG_A   44  GVRYNSLPGFFNRKAAEQSAAEVALRELAK------------------------------   73
2MDR_A   78  GRWFPAVCA-HSKKQGKQEAADAALRVLIGENEKAER------------------------------   113
1T4O_A   48  DGTVLGTGVGRNIKIAGIRAAENALRDKKMLDFYAKQRAAIPRSESVLKDPSQKNKKRKFSDTSHHHHHH   117
2CPN_A   58  --RFIEIGSGTSKKLAKRNAAMLRVSGPSSG------------------------------   89
2LJH_A   74  GQKY--LGQGRSKKVARIEAAATALRSFIQFKDGAVLSPLKPA------------------------------   114
2NUG_D1  43  --EYRTLGEGKSKKEAEQRAAEELIKLLEESE------------------------------   72
```

B

C

D

Figure S1: Rigidity profiles for all the dsRBDs in the multiple sequence alignment.
(**A**) Multiple sequence alignment for the dsRBD fold, most rigid residues are shown in bold red (rigid residues whose force constant lies right underneath the rigidity criterion are shown in bold orange). Consensus residues forming the folding nucleus are framed and shown in bold green. (**B**) Rigidity

profile for the dsRBD from X. laevis (1DI2). All force constant curves are in kcal mol-1 Å–2. **(C)** Cartoon representation of the dsRBD from X. laevis with the consensus nucleus residues shown as red sticks. The representation in (c) was prepared using Visual Molecular Dynamics. (D) Rigidity profile of various dsRBD. All force constant curves are in kcal mol^{-1} Å^{-2}.
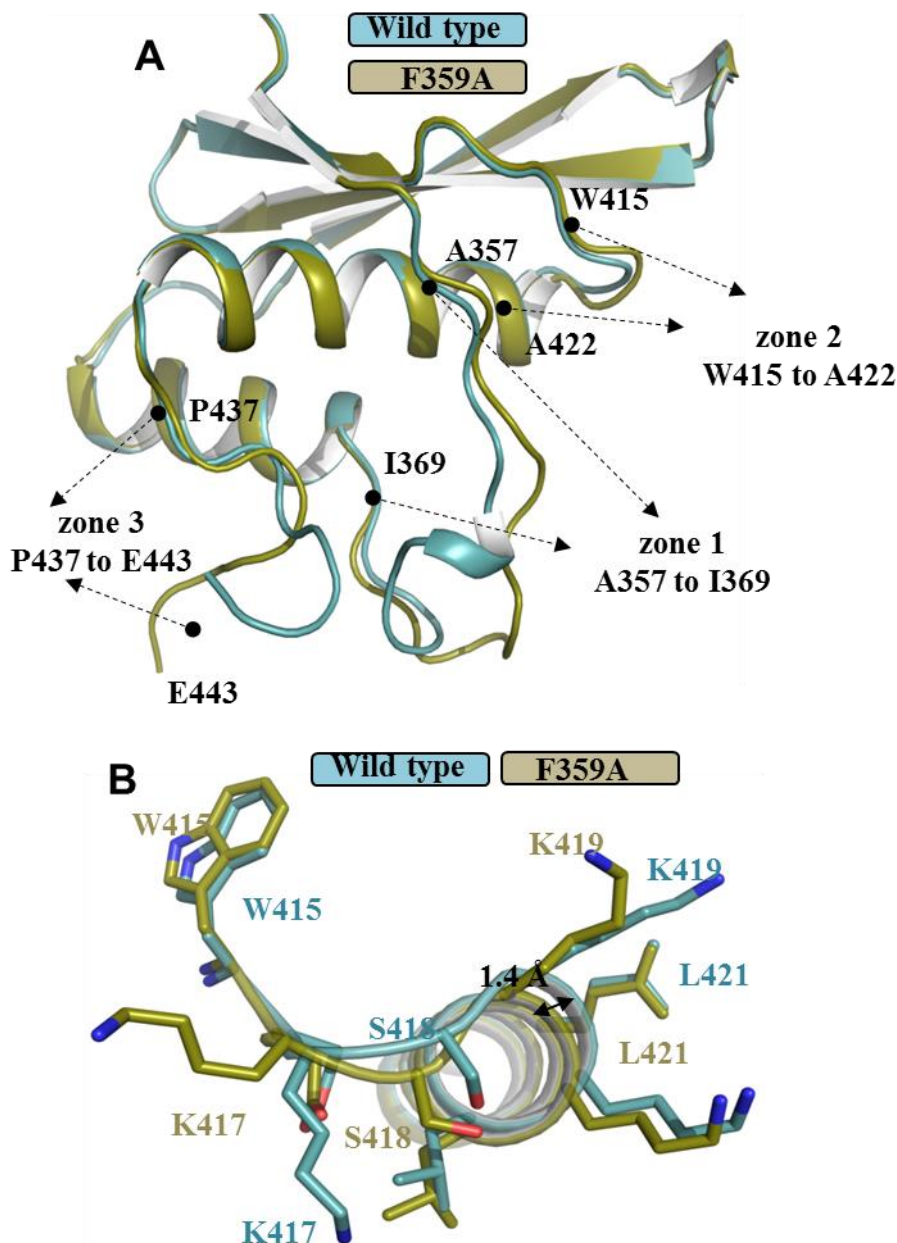

Figure S2: Structural comparison of wild type hDus2-dsRDB with its F359A mutant.
(**A**). Superposition of X-ray structures of wild type hDus2-dsRBD (blue, PDB: 4WFT) and F359A mutant (blue). Zones 1 to 3 delimitate the regions that have undergone structural changes following F359A mutation. (**B**) Structural alignment between wild type and F359A dsRBDs showing the perturbation induced by the mutation in the N-terminal region of helix α2.
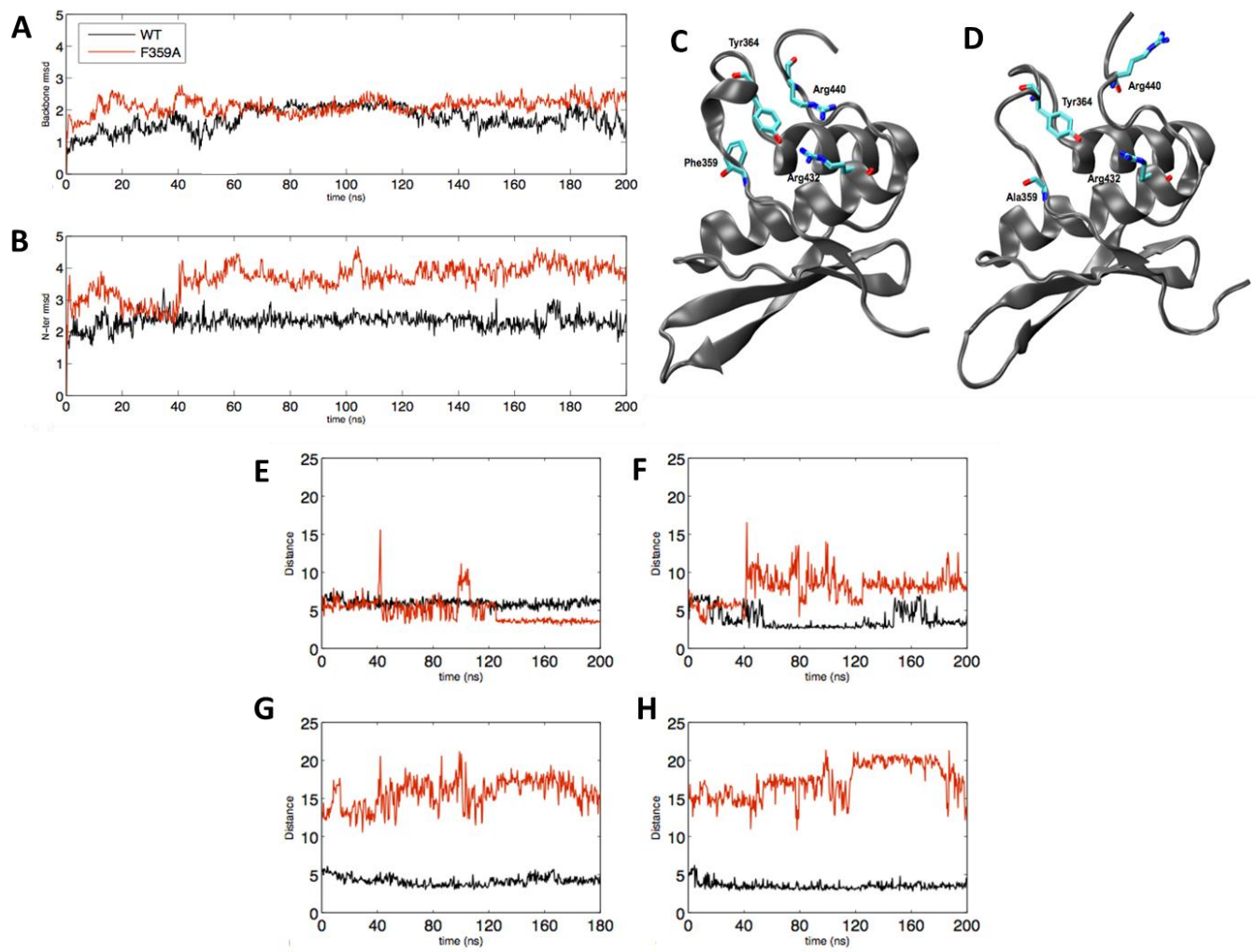
Figure S3: Conformational characterization of wild type and F359A dsRDBs by molecular dynamic.

(**A**), RMSDs (in Å) during 200 ns all-atom MD trajectories over the complete protein. (**B**), RMSD (in Å) over the N-terminal extension. Black line: Wild type dsRBD. Red line: F359A mutant. (**C**) and (**D**), are cartoon representation of dsRBDs with residues 359, 364, 432 and 440 shown as sticks for wild-type and F359A mutant, respectively. (**E-H**) are Interatomic distances (in Å) during the 200 ns all-atom MD trajectories, black line: wild-type protein, red line: F359A mutant. (e) Cα-Phe(Ala)359/Oη-Tyr364 (f) Oη-Tyr364/Nη$_2$-Arg440 (g) Oη-Tyr364/Nε-Arg432 (h) Nε-Arg432/Nη$_2$-Arg440.
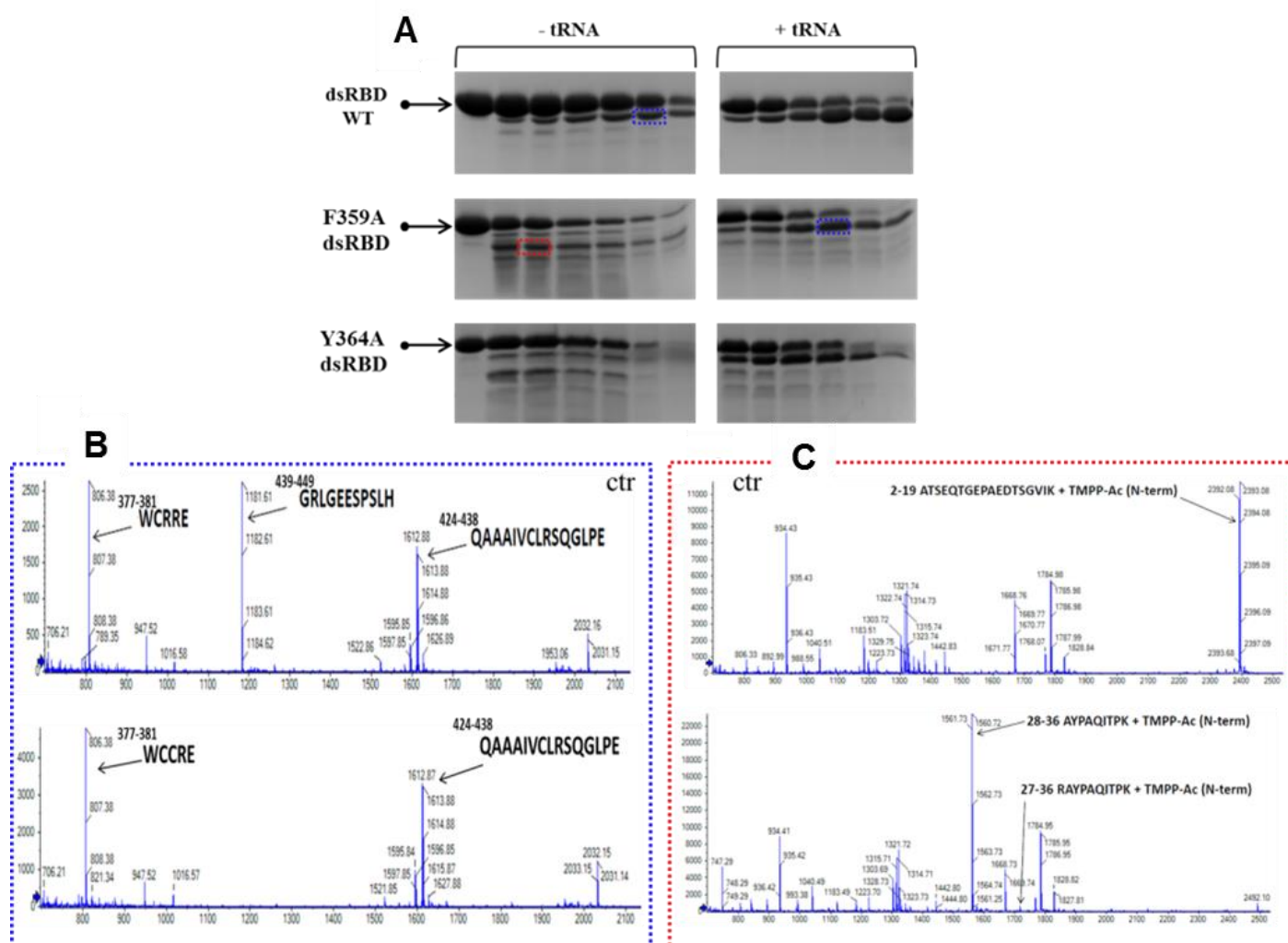
Figure S4: Structural characterization of dsRBD wild type, F359A and Y364A mutants.
(A) Mild trypsinolysis pattern of dsRBD and its mutants in the presence or absence of tRNA. In blue and red are highlighted the bands further analyzed by MALDI-MS. **(B)** Zooms of MALDI MS spectra of control undigested dsRBD (top panel) and Glu-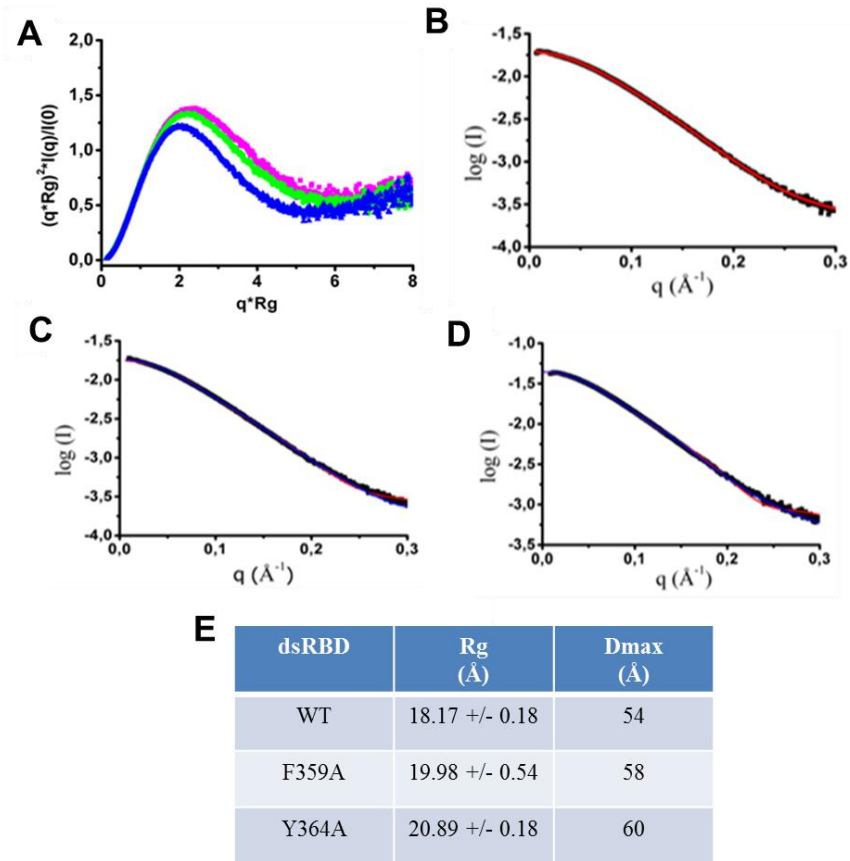C (low panel) proteolysis of blue band indicated in panel a. **(C)** Zooms of MALDI MS spectra of control undigested dsRBD F359A (top panel) and trypsin generated (low panel) proteolysis of red band indicated in panel a.

dsRBD	Rg (Å)	Dmax (Å)
WT	18.17 +/- 0.18	54
F359A	19.98 +/- 0.54	58
Y364A	20.89 +/- 0.18	60

Figure S5: SAXS characterization of dsRBD and its F359A and Y364A dRBD mutants.
(**A**) Normalized Kratky plot for dsRBD (blue), F359A dsRBD (green) and Y364A dsRBD (magenta).
(**B**), (**C**) and (**D**) are the superposition of the SAXS experimental curve (black) and theoretical scattering curve (red) of the wild type, F359A and Y364A dsRDB, respectively. (**E**) Table summarizing SAXS data used in this study.
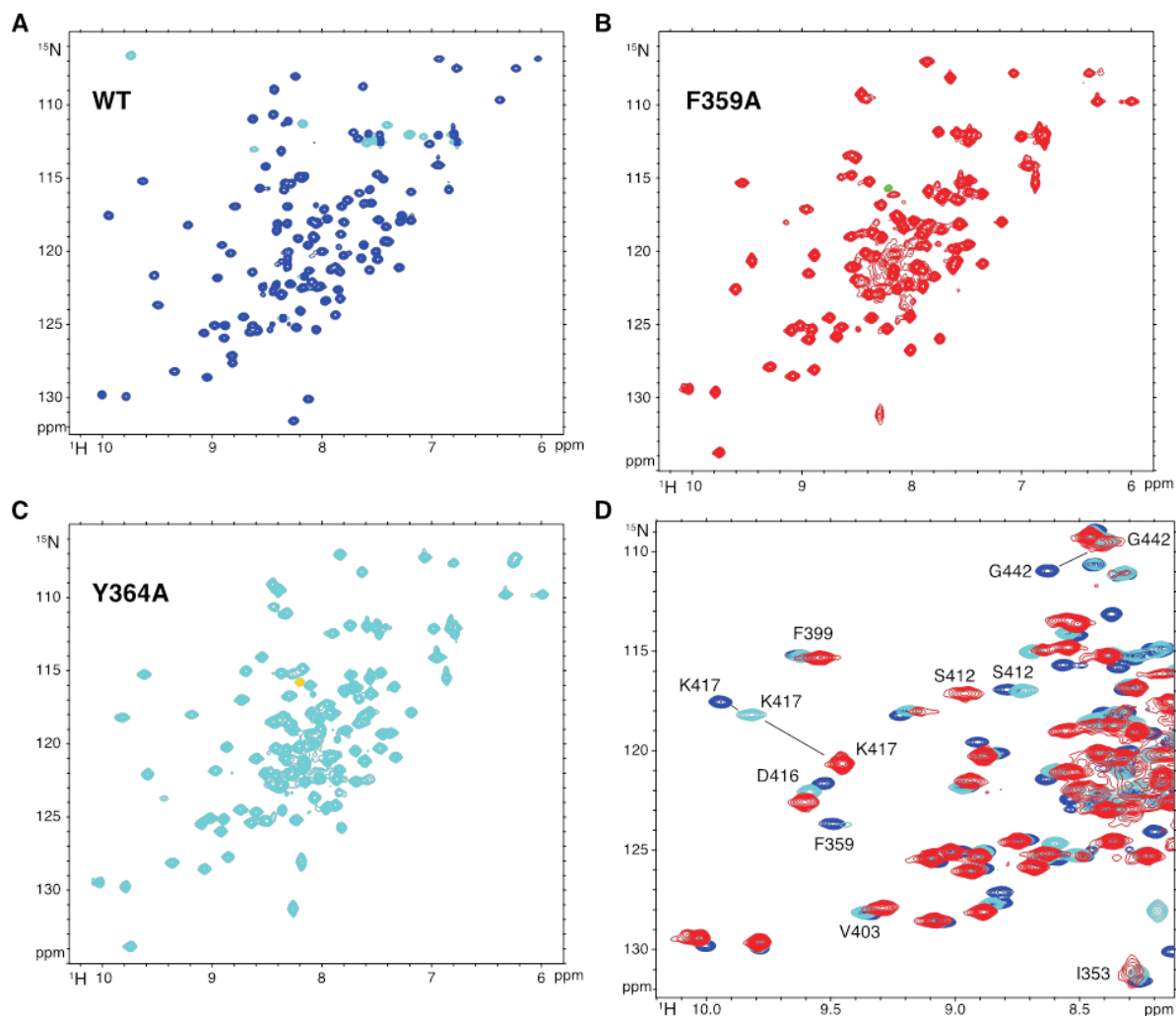
Figure S6: NMR spectra of the dsRBDs showing line broadening for certain residues in the mutants F359A and Y364A.

(A) (^{1}H,^{15}N)-HSQC of WT dsRBD. Aliased negative signals are in cyan. (B) (^{1}H,^{15}N)-HSQC of the F359A dsRBD mutant. Aliased negative signals are in green. (C) (^{1}H,^{15}N)-HSQC of the Y364A dsRBD mutant. Aliased negative signals are in yellow. (D) Overlay of the three (^{1}H,^{15}N)-HSQCs of panel A-C zoomed on a certain region of the spectra to show the line broadening of some signals. See for instance S412, F399, I353 and F359. Overall, line broadening is more pronounced in the F359A mutant than in the Y364A mutant. One can also appreciate the changes in the chemical shifts supporting structural changes beyond the NTE itself, see for instance the large chemical shift changes of K417 and G442 (see also Figure S7).
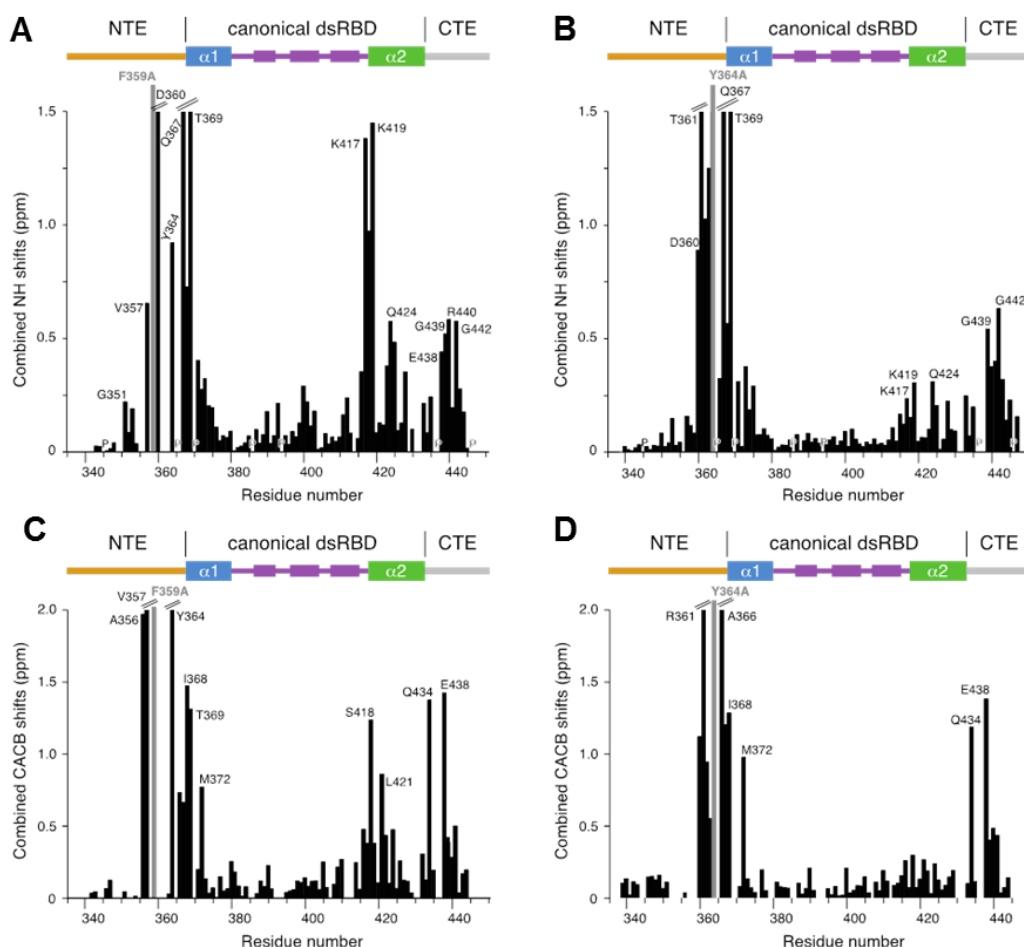
Figure S7: Chemical shift changes in F359A and Y364A dsRBD mutants.
(**A-B**) Chemical shift changes calculated as $[(\Delta\delta^{15}N/6.51)^2+(\Delta\delta^1H)^2]^{1/2}$ for F359A dsRBD mutant (**A**) and Y364A dsRBD mutant (**B**). The site of mutation is represented in grey. Missing values are from proline residues or residues with missing assignment in the wild-type and/or dsRBD mutants. The secondary structure of wild-type dsRBD is placed above the histogram. (**C-D**) Chemical shift changes calculated as $|\Delta\delta^{13}C\alpha|+|\Delta\delta^{13}C\beta|$ for F359A dsRBD mutant (**C**) and Y364A dsRBD mutant (**D**). The site of mutation is represented in grey. Missing values are from residues with missing assignment in the wild-type and/or dsRBD mutants. In case of glycine residues, only the $|\Delta\delta^{13}C\alpha|$ value is plotted. The secondary structure of wild-type dsRBD is placed above the histogram.
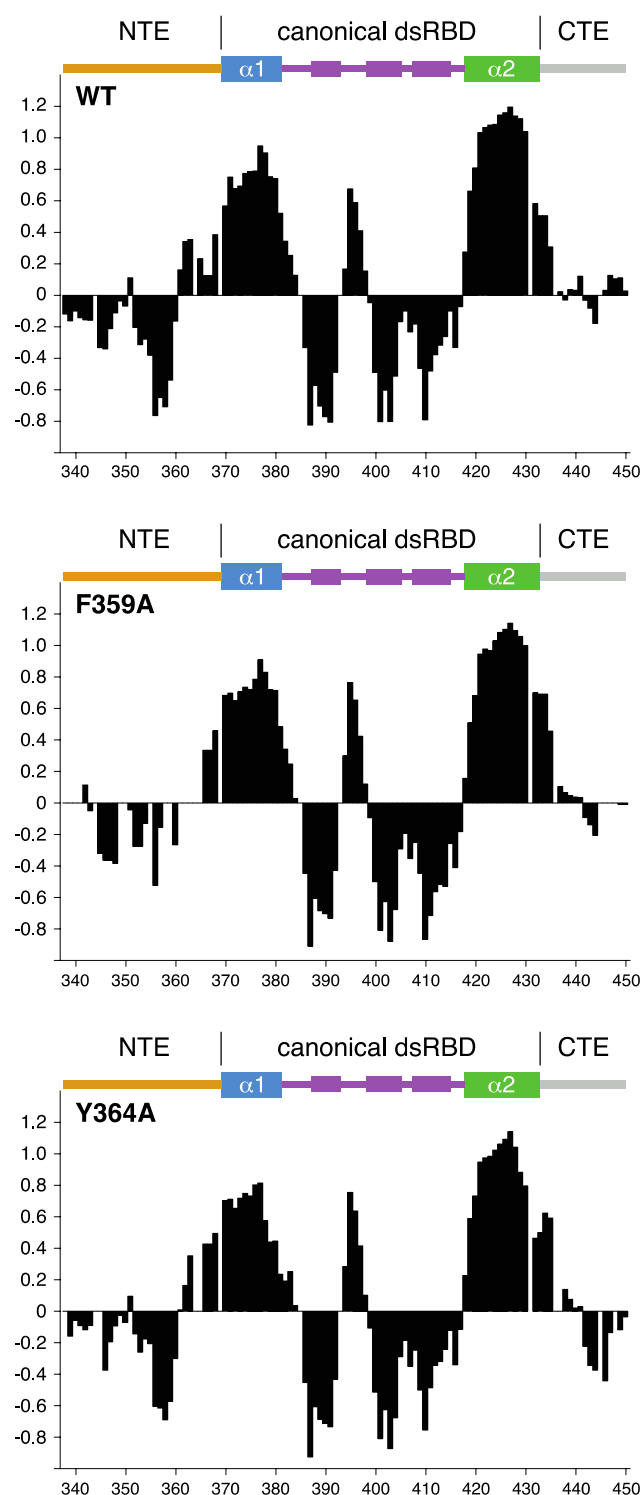
Figure S8: Secondary structure propensity of wild-type dsRBD, and the mutants F359A and Y364A.
Secondary structure propensities were calculated with the program SSP ([1]) with the automated carbon chemical shifts re-referencing and a max SSP score of 1.2. Cα, Cβ, HN and N chemical shifts were used as input data for the calculations. Positive values indicate a α-helical conformation, whereas

negative values indicate extended or β-strand conformations. The secondary structure of wild-type dsRBD (PDB code 4WFT) is placed above the histogram.

	hDus2-dsRBD F359A mutant PDB 6EI8
Data collection	
Space group	$P3_121$
Cell dimensions	
a, b, c (Å)	81.11, 81.11, 56.05
α, β, γ (°)	90, 90, 120
Resolution (Å)	43.81 – 2.25
	(2.33 – 2.25)
R_{sym} or R_{merge}	0.2345 (2.767)
R_{meas}	0.246 (2.89)
$CC_{1/2}$	0.996 (0.34)
I / σI	8.1 (0.9)
Completeness (%)	99.90 (100.0)
Redundancy	11.2 (11.6)
Refinement	
Resolution (Å)	43.81 – 2.25
No. reflections	10383 (1038)
R_{work} / R_{free}	0.259/0.286
No. atoms	
Protein	765
RNA	-
Ligand/ion	15
Water	48
B-factors	
Macromolecule	51. 01
Ligand/ion	77.88
Water	51.70
R.m.s. deviations	
Bond lengths (Å)	0.01
Bond angles (°)	1.08

Table S1: Summary of data collection and refinement statistics.

	ΔG^0 (kcal.mol^{-1})	m-value (kcal.mol^{-1}.M^{-1})	Cm (M)
dsRBD	3.3 ± 0.2	1.5 ± 0.1	2.2

	k_u^{H2O} (s^{-1})	$m_u^{\#}$ (kcal.mol^{-1}.M^{-1})	$k_u^{H2O}{}_{mut}$/ $k_u^{H2O}{}_{WT}$
Wild type	0.003 ± 0.0003	0.6 ± 0.07	-
ΔNTE	0.12 ± 0.02	0.6 ± 0.1	40
	1.3 ± 0.2	0.2 ± 0.03	433
F359A	0.054 ± 0.006	0.53 ± 0.07	18
Y364A	0.023 ± 0.003	0.6 ± 0.07	7.7

Table S2: Thermodynamic and kinetics parameters characterizing dsRDB stability, determined by urea-induced denaturation experiments.

References

1-Marsh,J.A., Singh,V.K., Jia,Z. and Forman-Kay,J.D. (2006) Sensitivity of secondary structure propensities to sequence differences between alpha- and gamma-synuclein: implications for fibrillation. Protein Sci., 15, 2795–2804.